Thermochimica Acta, 218 (1993) 401–411
Elsevier Science Publishers B.V., Amsterdam

Melting point and supercooling characteristics of molten salt

M. Yamada, M. Tago, S. Fukusako, and A. Horibe

Department of Mechanical Engineering, Hokkaido University, Sapporo 060, Japan

Keywords: molten salt, melting point, thermal storage, supercooling

ABSTRACT

Melting points of some kinds of molten salts have been determined, and also supercooling characteristics of potassium thiocyanate KSCN and calcium chloride $CaCl_2$ have been investigated. Molten salt has been utilized as a thermal storage material, cooling material for the nuclear reactor, refinement of the petroleum, fuel battery, molten-salt reactor because of its excellent thermal characteristics and chemical stability. Therefore, it is important for its utilization to store the data of thermophysical properties to control both the melting and solidification processes. The sample of molten salt is both heated and cooled depending on the prescribed heating-cooling temperature curves in the electric furnace with a controller. The melting points were determined as the constant temperatures which can be observed for some period in the cooling process. Furthermore, the supercooling characteristics were investigated under various sample masses and cooling rates as parameters. It was found that the degree of supercooling depended closely on both the cooling rate and the sample mass.

INTRODUCTION

Molten salts have, in general, excellent characteristics of thermophysical properties such as low vapor pressure, low viscosity, and high thermal capacity, and they do not decompose even in high temperature. Furthermore, they show chemical stability at high temperature. Therefore, molten salts have been utilized for the refinement of metal and petroleum, thermal processing of metal, and so forth.

Recently, molten salts have been expected for the utilization as the storage medium in high temperature chemical and thermal systems, such as for high temperature reactors (solar reactor, nuclear reactor, etc.), fuel batteries, and secondary batteries.

In the technical usage of molten salts, the information of thermophysical properties is indispensable, and it is required to store reliable data of thermophysical properties. For this purpose, the measurements of various kinds of thermophysical properties,

such as specific heat (Kobayashi et al. 1988, 1990), melting point, thermal conductivity (Nagasaka and Nagashima 1990, Nakazawa et al. 1990), thermal diffusivity (Araki et al. 1990), viscosity (Dumas 1970, Wakao et al. 1990), and thermal radiation properties (Makino et al. 1989) have been carried out.

In using molten salts as a thermal storage material, stable control of the melting–solidification phase change process is required. In general, supercooling, in which the material preserves the liquid condition below the equilibrium solidification temperature, is observed when the liquid solidifies. The supercooling is often observed in solidification of the molten salt such as alkali carbonate. Such a quasi–stable state is unfavorable for the utilization of the molten salts as a thermal storage material. Consequently, it is necessary to avoid or control this phenomenon. Therefore, it seems quite important not only to store data of thermophysical properties, but also to understand the melting–solidification process of the molten salts in detail.

In this report, measurements for the melting points of some kinds of molten salts are presented, and also the supercooling behavior for some molten salts under a variety of cooling rates and sample masses are determined.

EXPERIMENTAL APPARATUS AND PROCEDURES

Experimental apparatus

The schematic diagram of the measuring apparatus is depicted in Fig. 1. The apparatus consists fundamentally of a test cell, electric furnace, temperature control system, microcomputer, atmospheric gas refining system, vacuum pump, and associated instrumentation.

The sample is set into the test cell both to be heated and cooled in the electric furnace. The temperature in the electric furnace (200V–4.5kW, Max. Temp. 1600 °C) is controlled by a programmable temperature–controlling unit and a microcomputer.

Figure 2 shows the detail of the test cell. The sample crucible, for which the NC Tanmann tube is utilized, is installed in the quartz–glass tube (40 mm O.D., 36 mm I.D., 400 mm in length). The water jacket cap (Pyrex glass) is set at the top of the tube in order to control the atmosphere in the tube. The interior of the tube was kept under vacuum using the vacuum pump during the drying process of the sample.

To prevent for the samples from suffering a change in quality, the tube was filled with an inert gas such as argon or carbonic acid depending on the sample. The inert gas was supplied from a gas tank through the refinement loop. In the gas refinement loop, argon gas was both purified and dried by going through three Hartmann tubes which are filled with sulfic acid, calcium chloride, and magnesium perchlorate, respectively. For carbonic acid gas, the Hartmann tubes are filled with sulfic acid, silica gel, and diphosphorus pentoxide, respectively.

Platinum–rhodium thermocouples having a 0.5 mm diameter and sheathed in a protection tube were set into both the electric furnace and sample crucible. The thermocouples in the sample crucible was located at just center the sample, and that in the electric furnace was located at the middle point between the furnace wall and

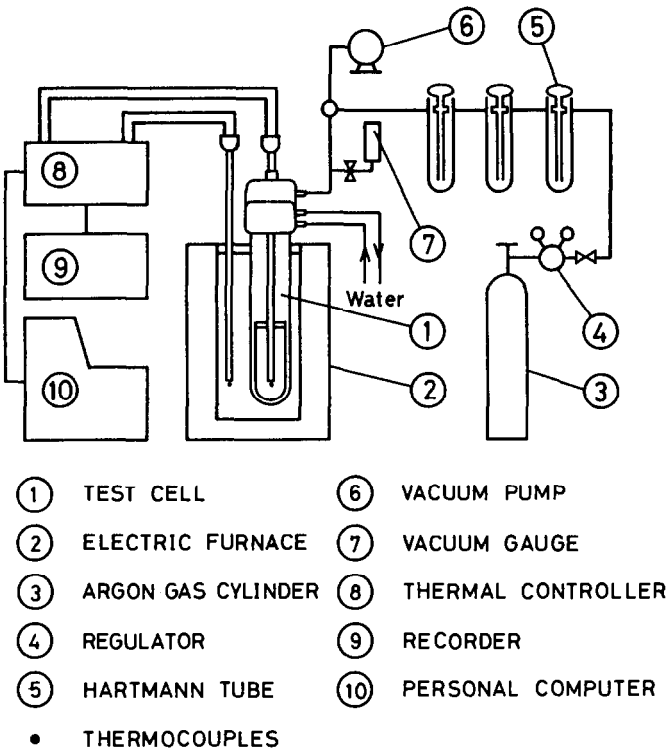

Fig. 1. Schematic diagram of apparaus

the test cell in the same horizontal level as the thermocouples in the sample crucible as shown in Figs. 1 and 2. The output of the thermocouples was recorded on a hybrid-recorder (YHP, TYPE-3088).

Procedures

In order to dehydrate the test sample, it was kept under both prescribed high temperature and vacuum pressure (1 to 15 torr). The conditions of drying treatment for the samples are respectively shown in Table 1. The atmospheric conditions during the measurement are also shown in the Table. The samples used in the present measurement are of special high quality.

In the measurements, in order to protect the sample from pollution and chemical reaction, the quartz-glass tube was filled with argon or carbonic acid gas, which had been purified and dried by going through the gas refinement loop.

The rate of temperature change in the electric furnace was controlled within the range of 1 to 7 °C/min. for each sample. In the observation of supercooling characteristics of the samples, the cooling rate of a sample could be varied from 0.8 to 18 °C/min.

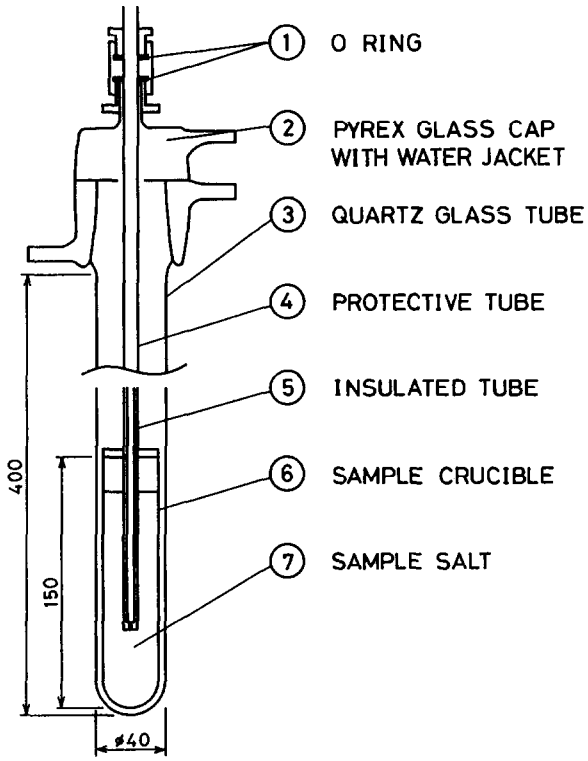

Fig. 2. Detail of test cell

RESULTS AND DISCUSSION

Melting point

In Figure 3, the temperature changes of both electric furnace and sodium sulfate Na_2SO_4 are demonstrated as an example of a heating–cooling curve. In the figure, curve No.1 denotes the temperature of the sample, and No.2 denotes that for the furnace. Some periods can be obsrerved where the temperature remains constant for both heating and cooling process. A constant value of temperature can be recognized as indicatig the melting point of the salt. There were some cases where the cooling equilibrium temperature did not coincide with the heating one due to the difference of the condition of the sample. In the present measurement, the constant temperature obtained in the cooling process was adopted as the melting point because the liquid condition after the melting is more homogeneous than the powder condition before the melting.

Measurement results of the melting points are summarized in Table 2 along with reference data. For every samples the present measurement results almost agree with the reference data, while being slight lower than the reference data except for the

TABLE 1

Drying treatment of sample

Sample	Drying treatment			Atmosphere during measurement
	Temp. (°C)	Time (hour)	Atmosphere	
$NaNO_2$	150	24	Vacuum (1 torr)	Argon Gas
$LiNO_3$	150	22		
$NaNO_3$	150	24		
KNO_3	120	24		
LiCl	450	22		
NaCl	500	24		
KCl	600	24		
Li_2CO_3	500	20	Vacuum (10 torr)	Carbonic Acid Gas
Na_2CO_3	500	20		
K_2CO_3	500	22		
KSCN	120	24	Vacuum (1 torr)	Argon Gas
$CaCl_2$	500	24		
$BaCl_2$	500	24		
LiBr	400	20	Vacuum (5 torr)	
Li_2SO_4	500	20	Vacuum (10 torr)	
Na_2SO_4	500	20	Vacuum (15 torr)	

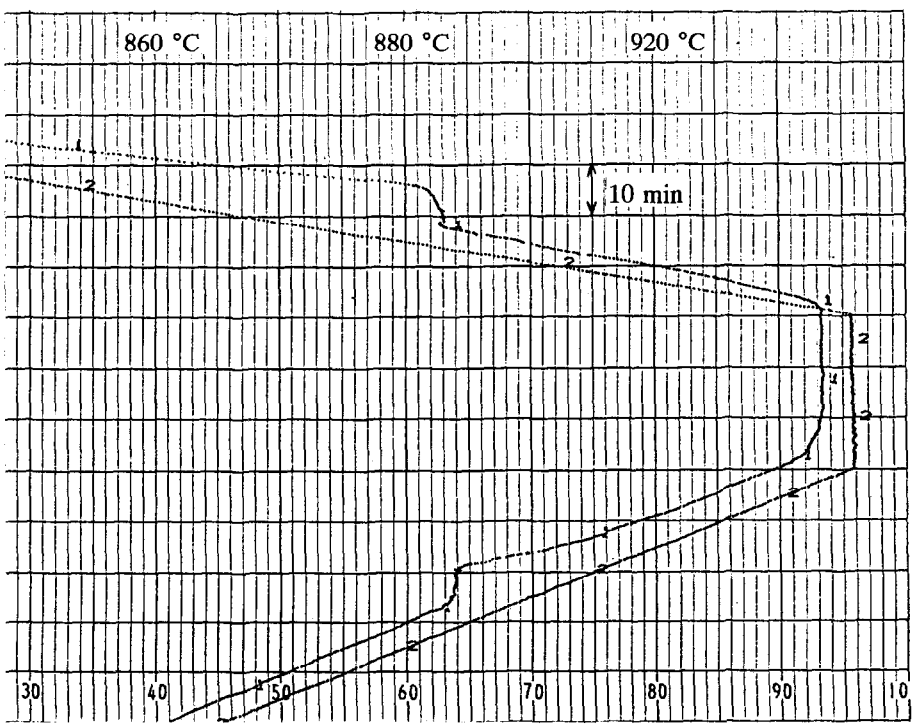

Fig. 3 Heating and cooling crve of Na_2SO_4

TABLE 2

Melting Point

	Melting Point (°C)			
Sample	Present Data	Literature[a]	Literature[b]	Literature[c]
$NaNO_2$	281		285	271
$LiNO_3$	252	253±2	254	
$NaNO_3$	305	307±1	310	306.8
KNO_3	334	337±1	337	333
LiCl	604	610±1	610	605
NaCl	800	800±2	800	801
KCl	768	770±1	768	770
Li_2CO_3	725	723±3	735	725
Na_2CO_3	860	858±1	854	851
K_2CO_3	903	893±3	895	891
KSCN	175			173
$CaCl_2$	773	782±5		772
$BaCl_2$	962	962±5		962
LiBr	548	552±3		
Li_2SO_4	854	859±3		
Na_2SO_4	886	884±2		884

[a] Janz et al., 1978
[b] JSME, 1986
[c] Iwanami Pub., 1987

carbonic acid salts.

Generally, measurement data of melting points can not be simply compared with each other because various factors such as purity of the sample, drying treatment, and sample mass will exert considerable effects on the melting point. In the present case it is considered that the suspension condition of the sample in the crucible, and heating or cooling process will cause the differences between the present data and the reference data.

It appears that convection in the molten sample in the crucible may occur and affect the temperature distribution in the sample for the present system. Therefore, it is very important to investigate both the flow pattern and solidification process by visualization.

Supercooling characteristics

In Figures 4 to 7 the effect of cooling rate on the supercooled temperature of potassium thiocyanate KSCN are indicated. The melting point of KSCN is 175 °C for the present measurement. The cooling rates for each figure are 0.8, 1.6, 2.7, and 3.7 °C/min, and the supercooled temperatures are 155, 159, 165, and 166 °C, respectively. As seen from the figures, the degree of supercooling increases as the

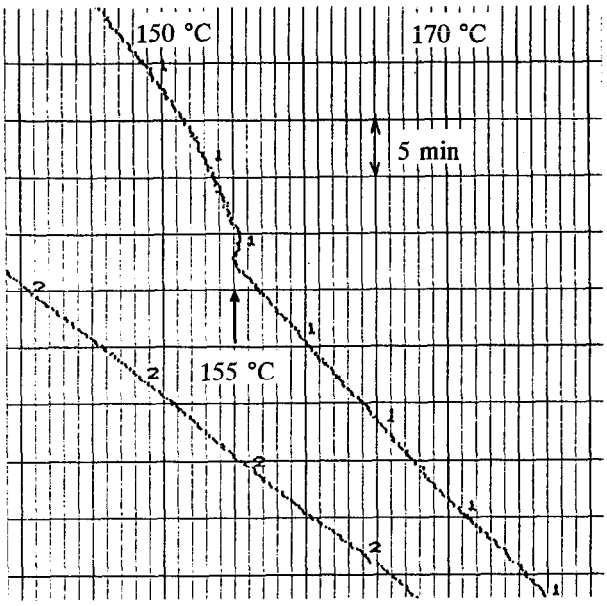

Fig. 4 Cooling curve of KSCN with cooling rate of 0.8 °C/min.

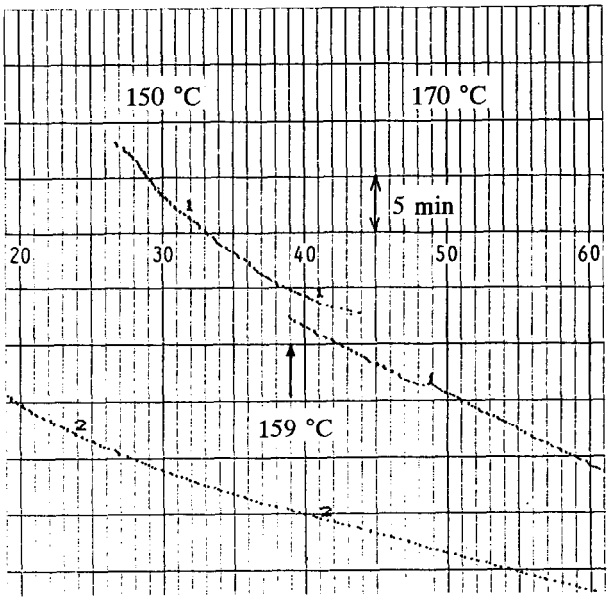

Fig. 5 Cooling curve of KSCN with cooling rate of 1.6 °C/min.

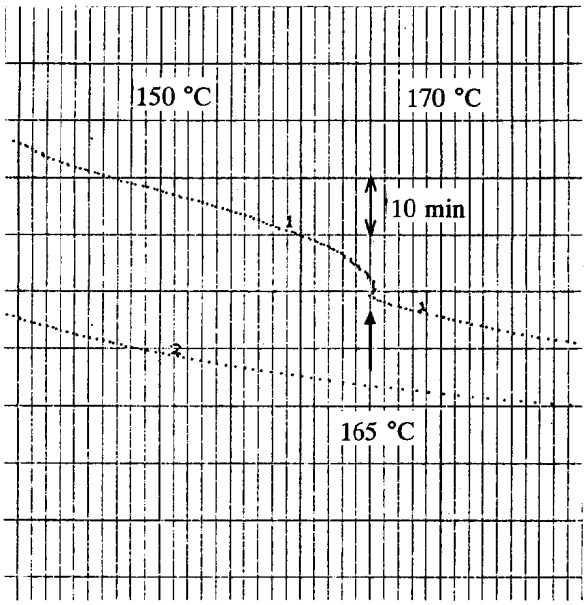

Fig. 6 Cooling curve of KSCN with cooling rate of 2.7 °C/min.

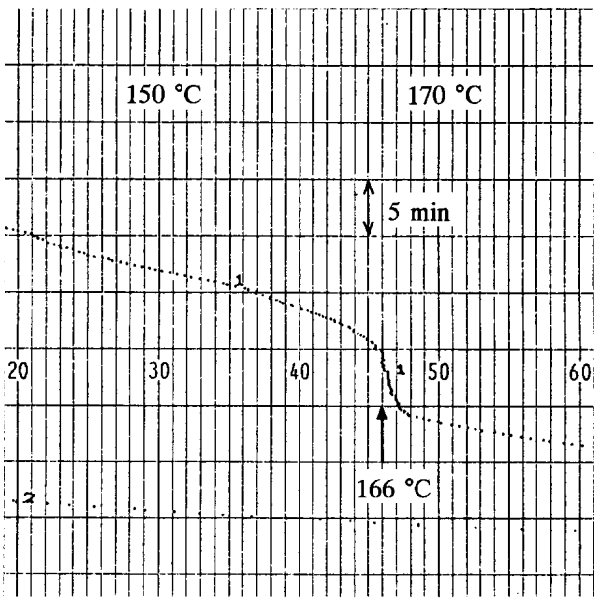

Fig. 7 Cooling curve of KSCN with cooling rate of 3.7 °C/min.

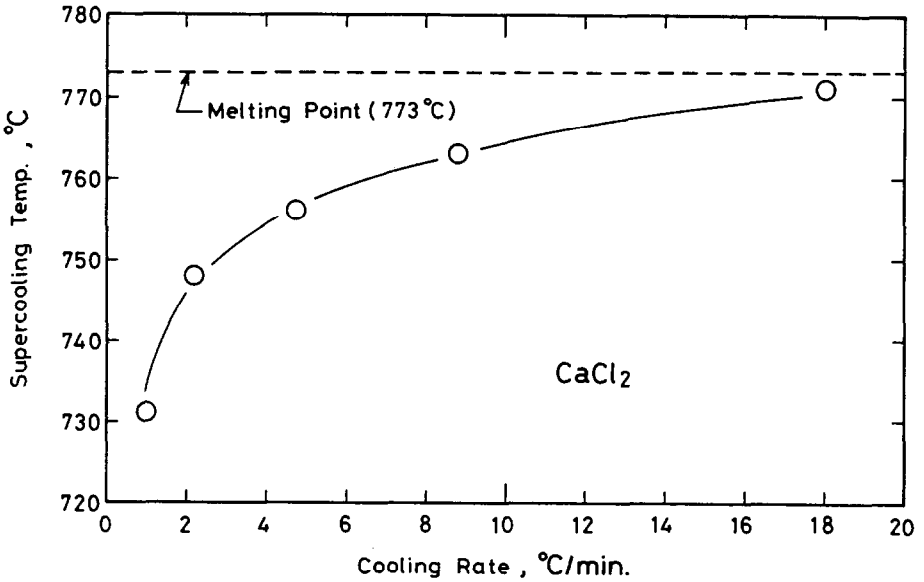

Fig. 8. Relationship between supercooling temperature and cooling rate

cooling rate decreases within the cooling rate range used for the present measurements.

The effect of cooling rate on the supercooling temperature for calcium chloride $CaCl_2$ is shown in Fig. 8. The abscissa denotes the supercooling temperature, while the ordinate shows the cooling rate of the sample. Similar to the case of KSCN, the degree of supercooling increases as the cooling rate decreases.

Figures 9 to 11 show the effect of sample mass on the supercooling temperature. The cooling rate was kept constant at 4.8 deg/min all through the experiments. An inspection of the figures reveals that the degree of supercooling increases as the sample mass decreases. It is widely held that the number of solidification nuclei decreases with a decrease in the sample mass, leading to an increase in the degree of supercooling. And it appears that the results of the present measurement may show the same tendencies.

CONCLUSIONS

Measurements of the melting points for some molten salts have been carried out. The supercooling characteristics of the molten salts have been further investigated. The measurement results were summarized and compared with reference data. The

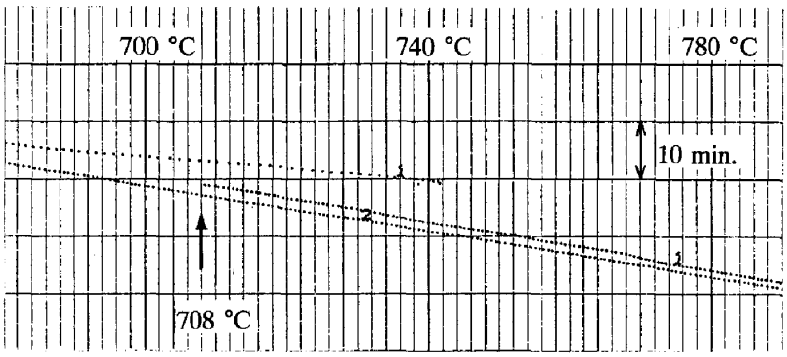

Fig. 9. Cooling curve of $CaCl_2$ with the sample weight of 13.5 g

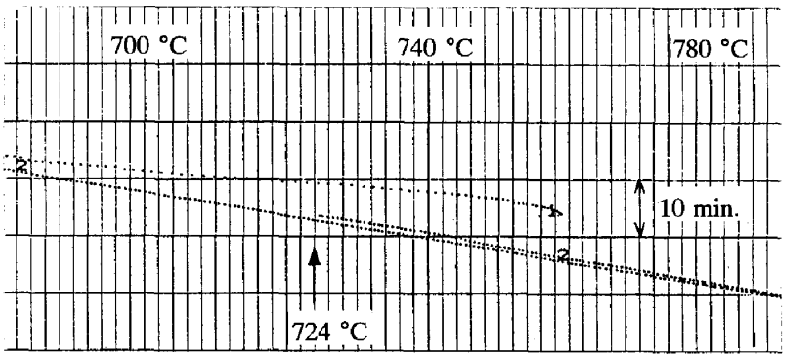

Fig. 10. Cooling curve of $CaCl_2$ with the sample weight of 27.0 g

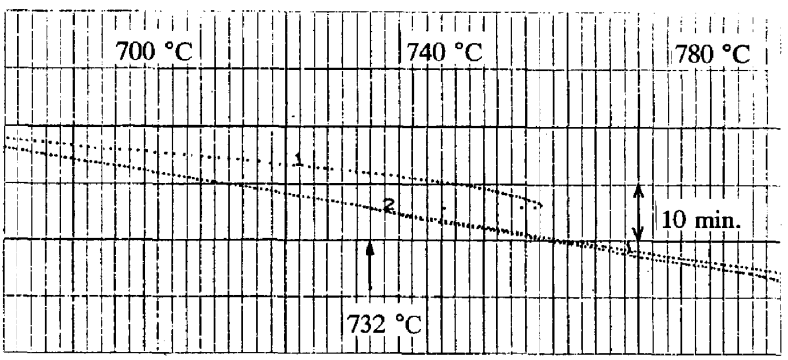

Fig. 11. Cooling curve of $CaCl_2$ with the sample weight of 40.5 g

following conclusions may be drawn within the range of the parameters covered in the present work.

(1) Measurement results of the melting point have some deviation ranges compared with other reference data, which may be mainly depending on the kind of molten salt sample due to the differences in purity, mass, and pre-treatment of the sample.
(2) The degree of the supercooling has a tendency to increase as both the sample mass and cooling rate decrease.

REFERENCES

Araki, N., Nakamura, Y., and Takano, Y., 1990, Effect of Rdiation Heat Transfer on Measurement of Thermal Diffusivity of Molten Salt by the Stepwise Heating Method, Proc. 11th JSTP: 263-266.

Iwanami Publish Co. Ltd, 1987, Rikagaku Jiten (in Japanese) 4th. Ed.

Janz, G. J., Allen, C. B., Donwey Jr., J. R., and Tomkins, R. P. T., 1979, Physical Properties Data Compilation Relevant to Energy Storage, NSRDS-NBS 61

Japan Soc. Mech. Engng., 1986, Technical Data Book:Heat Transfer 4th. Ed.: 324

Kobayashi, K., Inoue, N., and Koyama, Y., 1988, Measurement of Specific Heats of Solid and Molten Phases, and Latent Heat of Fusion of Some Carbonates, Proc. 9th. JSTP :111-114

Kobayashi, K., Inoue, N., and Takano, T., 1990, Measurement of Specific Heat of Solid and Molten Phases, and Latent Heat of Fusion of Some Carbonates (2nd. Report), Proc. 11th JSTP: 231-234

Makino, T., Maeda, T., Edamura, M, and Yoshida, A., 1989, Thermal Radiation Properties of Molten Alkaline Nitrates, 26th. Nat. Heat Transfer Sympo. Jpn.:184-186

Nagasaka Y. and Nagashima, A., 1990, Prediction of the Thermal Conductivity of Molten Alkali Halides by the Corresponding-States Correlation, Proc. of 11th. JSTP :275-278

Nakazawa, N., Akabori, M., Nagasaka, Y., and Nagashima, A., 1990, Measurement of the Thermal Diffusivity of Molten Salts by the Forced Rayleigh Scattering Method (Measurement of Molten Alkali metal Chlorides at Temperatures above 1000 °C), Trans. JSME B56:1467-1474

Sato Y. and Ejima, T., 1978, Phase Diagrams of $LiCl-AlCl_3$ and $NaCl-AlCl_3$ Binary System, Jour. Jap. Inst. Metals 42:905-912

Wakao, M., Ishito, S., Kojima, N., and Nagashima, A., 1990, Viscosity Measurement of Molten KCl and $NaBF_4$ by Oscilating-Cup Method - Recalculation of Temperature Dependences, Proc. 11th. JSTP :295-298